Characteristics of Activity Coefficient Models for Liquid Solutions

Philip T. Eubank and Xiaonian Wang
Dept. of Chemical Engineering, Texas A&M University, College Station, TX 77843

DOI 10.1002/aic.10081
Published online in Wiley InterScience (www.interscience.wiley.com).

Liquid–phase activity coefficient models (or excess Gibbs energy models) with three or fewer adjustable parameters are often sufficient to model the liquid solutions present for the vapor–liquid equilibria (VLE) or the vapor–liquid–liquid equilibria (VLLE) calculations of phase equilibria. Our purpose here is to show the flexibility of three such equations in the correlation and prediction of (1) extrema and inflection points on the popular ln γ_1 vs. x_1 diagram for binary solutions, (2) liquid–liquid phase splitting, and (3) homogeneous azeotropes. The empirical equations investigated here are (a) the two-constant Margules model, (b) the van Laar model, and (c) the three-constant NRTL model. New mathematical procedures lead to new graphs and equations, which allow the reader to identify the presence of any of the above three phenomena by inspection without performing detailed calculations such as a Gibbs energy minimization for liquid phase splitting. © 2004 American Institute of Chemical Engineers *AIChE J,* 50: 854–861, 2004
Keywords: vapor-liquid equilibria, liquid–liquid phase splitting, Margules, van Laar, NRTL

Introduction

Liquid–phase activity coefficient (γ_i) models (or excess Gibbs energy models, G^E/RT) with three or fewer adjustable parameters, dependent on temperature T, are often sufficient to model the liquid solutions present for the vapor–liquid equilibria (VLE) or the vapor–liquid–liquid equilibria (VLLE) calculations of phase equilibria (Gmehling and Onken, 1990). Our purpose here is to show the flexibility of three such equations in the correlation and prediction of (1) extrema and inflection points on the popular ln γ_i vs. x_1 diagram for binary solutions, (2) liquid–liquid phase splitting for binary solutions, and (3) homogeneous azeotropes for low pressures where gas-phase imperfections are unimportant. The empirical equations investigated here are (a) the two-constant Margules model, (b) the van Laar model, and (c) the three-constant NRTL model (Sandler, 1999; Smith, et al., 2001). We present new mathematical procedures and new graphs that allow the reader to identify the above three phenomena for the two-constant models of Margules and van Laar plus the three-constant NRTL. The graphical results are invaluable in determining quickly whether you will have, say, liquid–liquid phase splitting (or the other two phenomena listed above) for a given set of Margules, van Laar, or NRTL constants without performing detailed calculations.

It is important to understand the use of the Gibbs–Duhem equation with these models. In terms of the activity coefficients, the liquid–phase Gibbs–Duhem identity for a binary system is

$$(x_1)d\ \ln\ \gamma_1 + (x_2)d\ \ln\ \gamma_2 = [(V^E)/RT]dP - (H^E/RT^2)dT \quad (1)$$

where V^E and H^E are the excess volume and enthalpy, respectively, for the liquid solution. Here, we assume a binary system so the phase rule is simply $\mathcal{F} = 4 - \mathcal{P}$, where $\mathcal{F}$ is the number of intensive, independent variables required to fix the thermodynamic state and $\mathcal{P}$ is the number of phases. Then with a single-phase liquid solution, three independent variables (x_1, T, and P) are required to fix the state; we can vary x_1 at constant temperature and pressure, causing the righthand side (RHS) of

Correspondence concerning this article should be addressed to P. T. Eubank at p-eubank@tamu.edu.

the Gibbs–Duhem equation, Eq. 1, to be zero. A graph of ln γ_1 and of ln γ_2 vs. x_1 is highly restricted by Eq. 1 as

$$x_1(\partial \ln \gamma_1/\partial x_1)_{P,T} = -x_2(\partial \ln \gamma_2/\partial x_1)_{P,T} \quad (2)$$

requiring opposite signs for the two slopes. Any reasonable (G^E/RT) model of uniform continuity and zero at the pure end points obeys Eq. 2 at constant temperature and pressure—for a single liquid phase—because ln $\gamma_i = (\bar{G}_i^E/RT)$. The *constants* in the model are truly constant here because T and P are fixed.

In this article, we adhere to the notion of a single, liquid solution allowing for Eq. 2. However, the reader should be aware of the additional problems that arise when these models are applied to data from a VLE experiment (Eubank et al., 2000).

General Procedure

To generalize the results for all three events listed above, we have developed a procedure that can be applied to any excess Gibbs energy model *containing two model constants that are free to vary.* We denote these constants as A_{21} and A_{12} (as in the two-constant Margules model)—where $A_{12} \geq A_{21}$, by definition—which may redefine what is component 1 and component 2. We make this choice to define a parameter $r \equiv (A_{12}/A_{21})$, such that: (1) $r > 1$ when both constants are positive; (2) $0 < r < 1$ when both constants are negative; and (3) $r < 0$ only when the first constant is positive and the second is negative. Then all three events can be described and forecast in terms of r for a given value of A_{21}. In the first event of extrema and inflection points on the ln γ_i vs. x_1 diagram, which show a more complex type of deviation from an ideal solution, we simply rewrite the constants as above; find the model equations for ln γ_1 and ln γ_2; and, finally, take the first or second derivative, respectively, and set it to zero. However, the generalized procedures for the second and third events require further description as given in the next two sections.

Liquid Phase Splitting

We now present general results that apply to splitting of a single phase into two phases, here liquids from an excess Gibbs energy model. To see whether the liquid solution is more stable as two liquid phases, we need to examine the curve of the Gibbs energy of mixing ($\Delta_m G/RT$) vs. x_1 at constant temperature and pressure for the second derivative, which must remain positive for all x_1 if the liquid solution is to maintain single-phase stability for all values of the overall mole fraction z_1 representing one or more liquid phases. See Tester and Modell (1997) for an excellent discussion of the difference between equilibrium and phase stability.

Taking the second derivative of $g \equiv (\Delta_m G/RT) = x_1 \ln x_1 + x_2 \ln x_2 + (G^E/RT)$, we first check for inflection points, which occur as pairs, with the liquid–liquid immiscibility gap of (x_1^{II}, x_1^I) appearing outside the two inflection points. If a system of known overall composition falls inside this gap, L–L equilibria is stable, but if outside the gap, then single liquid phase is more stable. To find the equilibrium values of x_1^{II} and x_1^I it is necessary to examine the graph of g vs. x_1 and apply the tangent line method or, alternately, apply the equal-area rule (Eubank and Hall, 1995) to the graph of $g' \equiv (dg/dx_1)$ vs. x_1. These procedures work well with excess Gibbs energy models but must be applied *every time* we change the model constants.

Here we follow a less elegant, nongraphical procedure that correctly forecasts whether phase splitting occurs but without complete information as to the values of x_1^{II} and x_1^I. The fundamental criteria that $g'' = g''' = 0$ at the onset of phase splitting provides an algebraic equation between r and x_1(onset), after the elimination of A_{21} from the two equations that each contain A_{21}, r, and x_1 as variables. Next, this algebraic equation is used to eliminate x_1(onset) from the $g'' = 0$ equation, providing now r(min) vs. A_{21} or, alternately, A_{12}(min) vs. A_{21}. In an application where A_{21} and A_{12} are known (as in the two-constant Margules model), one can find A_{12}(min) and x_1(onset) for the fixed value of A_{21}. If the model value of A_{12} is less than A_{12}(min), then there is no phase splitting at any composition. When the model value of A_{12} is greater than A_{12}(min), there can be phase splitting, depending on the overall composition, whereas x_1^{II} and x_1^I are not known by this procedure, and some information is provided by x_1(onset). For example, when A_{12} is only slightly greater than A_{12}(min) and x_1(onset) is, say, 0.7, then we expect x_1^{II} and x_1^I to bound this value, say, 0.6 and 0.8. If the overall composition is 0.3, phase splitting is unlikely unless A_{12} is considerably greater than A_{12}(min). The net result is that this programmable nongraphical procedure can save one from the more involved tangent line process in most cases where there is no phase splitting. Especially in the form of the liquid–phase stability graph given here can one see immediately by inspection whether the more tedious procedure is necessary.

Homogeneous Azeotropes at Low Pressures

Here we present general results that apply at low pressures where the bubble-point curve of pressure vs. x_1 at constant temperature (or in the bubble-point curve of temperature vs. x_1 at constant pressure) is

$$P^{BP} = P_1^\sigma x_1 \gamma_1 + P_2^\sigma x_2 \gamma_2 \quad (3)$$

where both gas-phase imperfections and Poynting corrections have been ignored. To find a homogeneous azeotrope at constant temperature we differentiate Eq. 3 with respect to x_1 and set the derivative to zero. Equation 2 is the Gibbs–Duhem (G-D) form that applies for VLE when we ignore the V^E term for simplicity. Combination of this short form of the G-D equation with the differentiated form of Eq. 3 results in the azeotropic condition

$$\nu \equiv (P_1^\sigma/P_2^\sigma) = (\gamma_2/\gamma_1)^{AZ} \quad \text{or} \quad \ln \nu = \ln \gamma_2 - \ln \gamma_1 \quad (4)$$

The same equations applied at the pure-end-point limits, instead of to the azeotrope, further provide

$$(\partial P/\partial x_1)_T^\infty = P_2^\sigma(\nu\gamma_1^\infty - 1) \quad (5)$$

and likewise for the slope as x_1 approaches unity by interchanging the subscripts between the two components. Equation 5 is valuable because the sign of this slope at $x_1 = 0$ vs. its sign at $x_1 = 1$ provides information about whether an azetrope forms and whether the azeotrope is positive or negative.

It is important to remember that these VLE azeotropes cannot exist in the liquid–liquid immiscibility gap of (x_1^{II}, x_1^{I}) because as a single liquid phase is not stable with respect to two liquid phases.

Margules (Two-Constant) Model

This model originates as

$$(G^E/RTx_1x_2) = A_{21}x_1 + A_{12}x_2 \tag{6}$$

resulting in

$$\ln \gamma_1 = x_2^2[A_{12} + 2(A_{21} - A_{12})x_1]; \quad \ln \gamma_2 = x_1^2[A_{21} + 2(A_{12} - A_{21})x_2]; \quad \ln \gamma_1^{\infty} = A_{12}; \quad \ln \gamma_2^{\infty} = A_{21} \tag{7}$$

Extrema and inflection points

For the Margules model, Figure 1(a) shows a somewhat atypical graph of ln γ_1 and of ln γ_2 vs. x_1 corresponding to $r = 3$. In Figure 1(a), ln γ_2 has an inflection point at $x_1 = 0.42$, then undergoes a maximum at $x_1 = 0.83$ before falling back to A_{21} at $x_1 = 1$. In keeping with Eq. 2, ln γ_1 is zero at $x_1 = 0.75$, falling to its minimum at $x_1 = 0.83$, and then an inflection point at $x_1 = 0.92$, as better seen in Figure 1(b), a magnification of Figure 1(a). To find the general equations that forecast such behavior for any value of the ratio of Margules constants r, we need only take the first and second derivatives of Eq. 10 for each ln γ_1 and ln γ_2 and then set the results to zero. By Eq. 2, when ln γ_1 undergoes a maximum, ln γ_2 must experience a minimum or vice versa.

The following equations result for the Margules (two-constant) model:

For the maximum/minimum or extrema condition

$$x_1^M = \left[\frac{2r - 1}{3(r - 1)}\right] \tag{8}$$

For the inflection point in ln γ_1 and ln γ_2, respectively

$$x_1^{IP1} = \left[\frac{5r - 4}{6(r - 1)}\right] \quad x_1^{IP2} = \left[\frac{2r - 1}{6(r - 1)}\right] \tag{9}$$

Figure 2 is a graph of these special values of x_1 vs. r, reflecting that $x_1 \xi (0, 1)$. Extrema in the ln γ_i cannot occur for $r \xi (0.5, 2)$, whereas inflection points in ln γ_1 cannot occur for $r \xi (0.8, 2)$ and for ln γ_2 they cannot occur for $r \xi (0.5, 1.25)$. These results, and those below for the formation of a homogeneous azeotrope, are independent but both are invalid in a region of x_1, where the single liquid phase splits into two liquid phases. Figure 2 demonstrates part of the versatility of the Margules model and that it can provide *qualitatively* most of the general behavioral patterns of real liquid solutions—or at least those given in Abbott and Prausnitz (1994) and the most recent edition of Smith et al. (2001; their Fig. 12.9). Results for Porter's symmetric model (Margules single constant) with $r = 1$ show that extrema and inflection points cannot form.

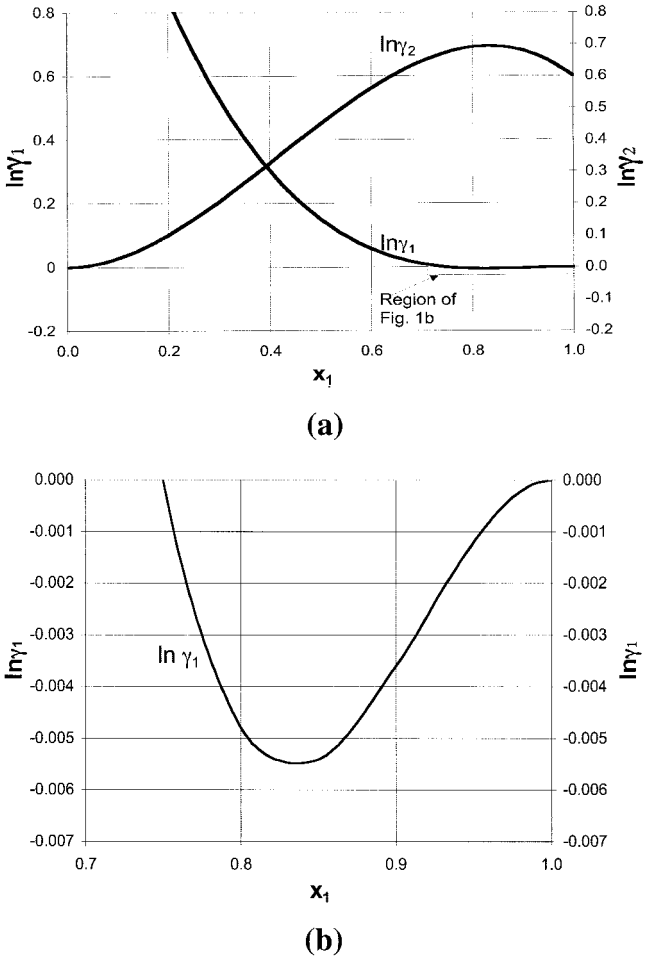

Figure 1. (a) Graph of ln γ_1 and of ln γ_2 vs. x_1 for the Margules model with $A_{12} = 1.8$ and $A_{21} = 0.6$.

In keeping with Eq. 8, ln γ_1 has a minimum of near -0.0055 at $x_1 = 0.83$, with ln γ_2 having a maximum at the same mole fraction as dictated by Eq. 2. From Eq. 9, ln γ_2 has an inflection point at $x_1 = 0.42$ and ln γ_1 has an inflection point at $x_1 = 0.92$. (b) Insert of region of (a) where ln γ_1: (a) passes through zero, (b) reaches its minimum value near $x_1 = 0.83$, and (c) has an inflection point near $x_1 = 0.92$.

Liquid–liquid phase splitting

By following the nongraphical procedure described above (Liquid Phase Splitting section), one obtains

$$2x_1x_2[3x_1(1 - r) + (2r - 1)] = (A_{21})^{-1} \tag{10}$$

from $g'' = 0$ at the *onset* of phase splitting, where the inflection points first appear at the same point. Combination of Eq. 10 with a second equation from $g''' = 0$, followed by elimination of A_{21}, results in

$$x_1^{onset} = \left[\frac{(5r - 4) - \sqrt{7 - 13r + 7r^2}}{9(r - 1)}\right] \tag{11}$$

Insertion of this value of x_1 into Eq. 10 and solving for $r = r_{MIN}$ as a function of A_{21} yields the left-ordinate curve of Figure 3 as $A_{12}(\text{min}) = A_{21}r_{MIN}$. This value of r_{MIN} then provides x_1^{onset}

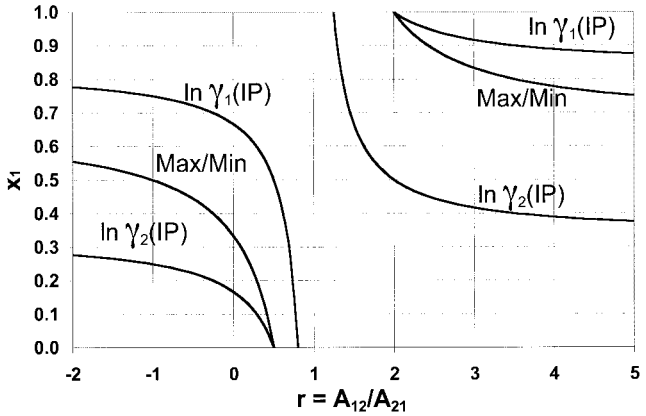

Figure 2. Margules locus lines for extrema and inflection points on ln γ_i vs. x_1 graphs with $A_{12} > A_{21}$.

from Eq. 10 for the right-ordinate curve of Figure 3. All values of x_1^{onset} are <0.5 because $A_{12} > A_{21}$. For $A_{21} < 2$, Figure 3 allows the reader to (1) determine whether phase splitting occurs and (2) when it does occur [$A_{12} > A_{12}$(min)], to know roughly that the liquid–liquid immiscibility gap of (x_1^{II}, x_1^{I}) is centered near x_1^{onset} with the magnitude of the gap increasing with [$A_{12} - A_{12}$(min)].

The above procedure works well when $A_{21} < 2$ and $A_{12} > 2$, but fails when both Margules constants exceed two, where phase splitting must occur, but the liquid–liquid immiscibility gap of (x_1^{II}, x_1^{I}) is generally wide. Then the tangent line method or, alternately, the equal-area rule must be applied for the given values of the two Margules constants.

For Porter's symmetric model, Eq. 10 provides the necessary working result, whereas the indeterminate Eq. 11 requires application of L'Hospital's rule for the correct but trivial result of 0.5. Further, when A varies with T so that (dA/dT) is positive for some temperature for which $A = 2$, we have a *lower critical solution temperature* (LCST), whereas a decreasing value of A as it passes through 2 provides an *upper critical solution temperature* (UCST) (Prausnitz et al., 1999).

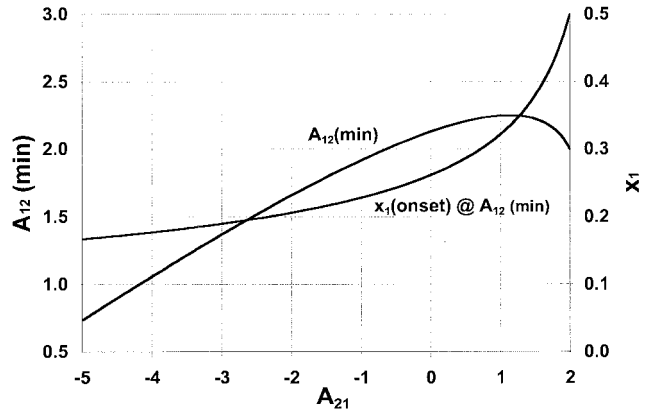

Figure 3. Margules locus lines for liquid–liquid phase splitting with $A_{12} > A_{21}$.

A_{12} (min) is the minimum value of A_{12} for which the single-phase liquid splits into two liquid phases for a given value of A_{21}. x_1(onset) is the mole fraction at which this splitting first occurs at A_{12} (min).

Homogeneous azeotropes

Equation 4 applied to Eq. 7 results in the quadratic equation

$$3(r-1)x_1^2 - 2(2r-1)x_1 + (\tau + r) = 0$$

$$x_1 \equiv x_1^{AZ}; \quad \tau \equiv [\ln(P_1^\sigma/P_2^\sigma)]/A_{21} \quad (12)$$

We arbitrarily chose to divide by the lower value of A_{21} rather than A_{12} for consistency with our definition of r. Some combined parameter of this type is required if the results are to be presented on two-dimensional graphs with r and τ as the coordinates. Note that the vapor pressure of the first component may be higher or lower than that of the second component because we are selecting component 1 so that $A_{12} > A_{21}$.

For $x_1 \xi (0, 1)$, we first examine the solution when $x_1 = 0$, finding $\tau = \tau_{MIN} = -r$, followed by the solution when $x_1 = 1$, finding $\tau = \tau_{MAX} = 1$; these results may be compared with Eq. 10 where $-1 \le \tau \le 1$ for the symmetric solution where $r = 1$. These results are shown in Figure 4, where *between* the straight lines of $\tau = -r$ and $\tau = 1$ a maximum is found in the pressure for $r < -1$, whereas a minimum is found in the pressure for $1 > r > -1$ and a maximum is again seen for $r > 1$; these correspond (Rowlinson and Swinton, 1982) to positive azeotropes (minimum boiling-point azeotropes), followed by negative azeotropes (maximum boiling-point azeotropes), followed by again positive azeotropes. The regions outside these lines in Figure 4 are more complicated and interesting. The solution of the quadratic Eq. 12 is complex when $3(r-1)(\tau + r) > (2r-1)^2$ or

$$\tau_M \equiv \left[\frac{r^2 - r + 1}{3(r-1)}\right] \quad (13)$$

where τ_M is the maximum value of τ for $r < 1$ but its minimum value for $r > 1$ each defining a region of complex solutions on Figure 4. If we set r and plot P^{BP} vs. x_1 with a computer graphics software that uses τ as a parameter, these complex solution regions are found to contain no azeotropes.

Likewise, there are no azeotropes in the regions marked *No Extrema* on Figure 4 but there are two regions where *double azeotropes* occur marked *Max/Min* [Positive/Negative

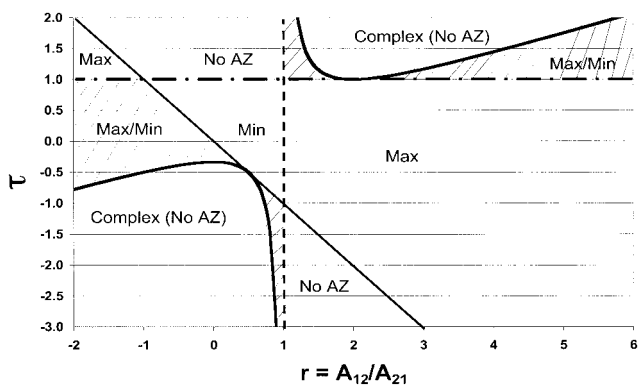

Figure 4. Margules regions for the formation of single and double azeotropes, with $A_{12} > A_{21}$.

Here, $\tau \equiv [\ln(P_1^\sigma/P_2^\sigma)]/A_{21}$. The regions where double azeotropes occur are hatched.

Azeotrope], depending on which azeotrope appears first with increasing x_1. Double azeotropy is rare in nature, usually occurring near a Bancroft point (where the pure-component vapor pressure curves cross or, here, where τ is zero). The Margules model is forecasting a Positive/Negative azeotrope for $r < 0.5$ depending on τ. When τ is near zero, r is less than zero or $A_{21} < 0$, whereas $A_{12} > 0$; thus Margules constants of opposite sign can lead to a double-azeotrope forecast whenever τ is roughly in the range of about -0.4 to 1. Likewise, when both Margules constants are positive with $r > 2$, a Positive/Negative azeotrope is forecast when τ is slightly above unity, as seen better in Figure 4. See Rowlinson and Swinton (1982) and, especially, van Konynenburg (1968) for more details about double azeotropy.

For Porter's symmetry model, Eq. 12 reduces to the more familar result of $(\tau + 1) = 2x_1$ at the azeotrope. Azeotropes are then present for values of τ between -1 and 1 (see also Figure 4 when $r = 1$).

van Laar Model

This model originates as

$$\left[\frac{x_1 x_2}{G^E/RT}\right] = (x_1/\beta) + (x_2/\alpha) \tag{14}$$

resulting in

$$\ln \gamma_1 = \alpha\left[\frac{x_2}{x_2 + (\alpha/\beta)x_1}\right]^2 \quad \ln \gamma_2 = \beta\left[\frac{x_1}{x_1 + (\beta/\alpha)x_2}\right]^2$$

$$\ln \gamma_1^{\infty} = \alpha \quad \ln \gamma_2^{\infty} = \beta \tag{15}$$

Consistent with the Margules analysis above, we chose the first component to be the one for which $\alpha \geq \beta$ in the van Laar model. This defines a parameter $r \equiv (\alpha/\beta)$, such that (1) $r > 1$ when both constants are positive, (2) $0 < r < 1$ when both constants are negative, and (3) $r < 0$ only when the first constant is positive and the second is negative. Details presented in the Margules section are not repeated here, where we concentrate on what is different between Margules and van Laar. The results follow exactly the sequence of the previous Margules analysis.

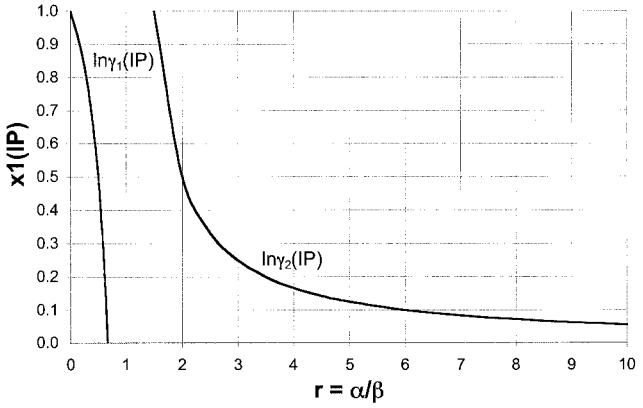

Figure 5. van Laar locus lines for inflection points on ln γ_i vs. x_1 graphs with $\alpha > \beta$.

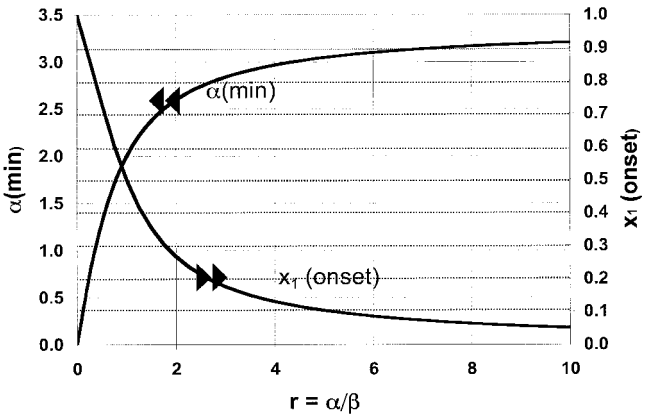

Figure 6. van Laar locus for liquid–liquid phase splitting with $\alpha > \beta$.

α(min) is the minimum value of α for which the single-phase liquid splits into two liquid phases for a given value of β. x_1(onset) is the mole fraction at which this splitting first occurs at α(min).

Extrema and inflection points

The van Laar model provides no extrema for ln γ_1 or ln γ_2 vs. x_1, except the trivial cases required by Eq. 2 for $x_1 = 0$ (for ln γ_2) and for $x_1 = 1$ (for ln γ_1). The inflection points in ln γ_1 and ln γ_2, respectively, are

$$x_1^{IP1} = \left[\frac{3r - 2}{2(r - 1)}\right] \quad \text{and} \quad x_1^{IP2} = \left[\frac{1}{2(r - 1)}\right] \tag{16}$$

Figure 5 shows that an inflection in ln γ_1 can occur only when the ratio r is between zero and unity, meaning that one van Laar constant is positive and the other negative. For ln γ_2, the inflection occurs only when the ratio r exceeds 1.5.

Liquid–liquid phase splitting

The fundamental criteria that $g'' = g''' = 0$ at the onset of phase splitting results in a quadratic relation between the ratio r and x_1(onset), which has the solution

$$(1 - r)x_1 = -r + \sqrt{r^2 - r + 1} \tag{17}$$

Equation 17 provides values of x_1(onset) from 0.5 when $r = 1$ (actually Eq. 17 is indeterminate) to near zero for large values of r, as seen in Figure 6. For $r = 0$, x_1(onset) is unity, so for $0 < r < 1$, x_1(onset) varies from unity back to 0.5. The value of α(min) is then given by

$$\alpha(\min) = \left[\frac{rx_1 + (1 - x_1)}{2x_1(1 - x_1)[1 + (1 - 2x_1)\psi - x_1(1 - x_1)\psi^2]}\right]$$

$$\psi \equiv \left[\frac{r - 1}{1 + (r - 1)x_1}\right] \tag{18}$$

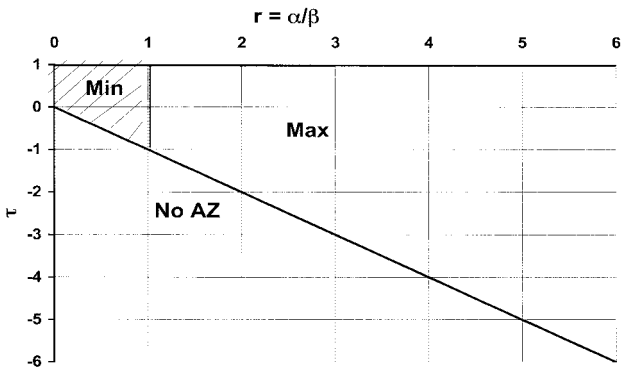

Figure 7. van Laar regions for the formation of single, homogeneous azeotropes, with $\alpha > \beta$.

Here, $\tau \equiv [\ln(P_1^\sigma/P_2^\sigma)]/\beta$. The regions where the negative azeotropes (min) occur are hatched.

Figure 6 also provides the values for α(min) as a function of r.

Homogeneous azeotropes

Equation 4 applied to Eq. 15 results in a quadratic equation with the solution

$$\left[\frac{(\tau + r)(1 - x_1)}{rx_1}\right] = -\tau + \sqrt{(r-1)\tau - r}$$

$$x_1 \equiv x_1^{AZ}; \quad \tau \equiv [\ln(P_1^\sigma/P_2^\sigma)]/\beta \quad (19)$$

The parameter τ is analogous to that defined in Eq. 12 for the Margules model. However, Figure 7 shows that the results for van Laar are very different from those of Figure 4 for Margules. Although the major division line of $\tau = -r$ is common, now any negative value of r produces a divergence of pressure on the P vs. x_1 diagram at $x_1 = (1 - r)^{-1}$. Further, there can be no homogeneous azeotropes for $\tau > 1$. Thus, Figure 7 is bounded by $r = 0$ and $\tau = 1$ in the upper left corner.

NRTL Model

This *nonrandom, two-liquid* model originated with H. Renon as described by Prausnitz et al. (1999). The equation is

$$(G^E/RTx_1x_2) = \left[\frac{\tau_{21}\exp(-\alpha_{12}\tau_{21})}{x_1 + x_2\exp(-\alpha_{12}\tau_{21})}\right] + \left[\frac{\tau_{12}\exp(-\alpha_{12}\tau_{12})}{x_2 + x_1\exp(-\alpha_{12}\tau_{12})}\right] \quad (20)$$

resulting in

$$\ln\gamma_1 = x_2^2\left\{\left[\frac{\sqrt{\tau_{21}}\exp(-\alpha_{12}\tau_{21})}{x_1 + x_2\exp(-\alpha_{12}\tau_{21})}\right]^2 + \left[\frac{\tau_{12}\exp(-\alpha_{12}\tau_{12})}{[x_2 + x_1\exp(-\alpha_{12}\tau_{12})]^2}\right]\right\}$$

and

$$\ln\gamma_2 = x_1^2\left\{\left[\frac{\sqrt{\tau_{12}}\exp(-\alpha_{12}\tau_{12})}{x_2 + x_1\exp(-\alpha_{12}\tau_{12})}\right]^2 + \left[\frac{\tau_{21}\exp(-\alpha_{12}\tau_{21})}{[x_1 + x_2\exp(-\alpha_{12}\tau_{21})]^2}\right]\right\} \quad (21)$$

As seen, the NRTL model has three parameters (τ_{12}, τ_{21}, and α_{12}) but α_{12}, a measure of nonrandomness of the mixture, is generally found to be between 0.2 and 0.47, with 0.3 as a typical value. When $\alpha_{12} = 0$, the model reduces to the symmetric model. The model is considered to be especially valuable for highly nonideal solutions that lead to phase splitting. Renon and Prausnitz (1969) provide graphs for determination of NRTL parameters from immiscibility data and from infinite dilution activity coefficients. Here we provide essentially the opposite result: given a set of NRTL parameters will one see phase splitting, homogeneous azeotropes, plus extrema and inflections points for $\ln\gamma_i$? Again we follow the same format as above for Margules and van Laar.

Extrema and inflection points

The NRTL model provides for extrema in the graphs of $\ln\gamma_1$ or $\ln\gamma_2$ vs. x_1 according to the formula

$$x_1^M = \left\{\frac{\exp[(2\alpha_{12}/3)(r-1)\tau_{21}] + r^{1/3}\exp(-\alpha_{12}\tau_{21})}{[-1 + \exp(-\alpha_{12}\tau_{21})]\{r^{1/3} - \exp[(2\alpha_{12}/3)(r-1)\tau_{21}]\}}\right\}$$

$$r \equiv (\tau_{12}/\tau_{21}); \quad \tau_{12} > \tau_{21} \quad (22)$$

We hoped to provide graphs similar to Figure 2 for several fixed values of α_{12} but Eq. 22 shows that use of r is not successful in elimination of the two parameters that make up its ratio, as was the case in Margules and van Laar. Extensive tests on a graphing calculator with x_1^M vs. r for different values of both α_{12} and τ_{21} revealed the following results: (1) there are no extrema for $r > 0$; (2) there are no multiple extrema; (3) for $|\alpha_{12}\tau_{21}| < 0.1$ with $\tau_{21} < 0$, extrema tend to appear near $r = -1$; (4) for $0.1 < |\alpha_{12}\tau_{21}| < 0.25$ with $\tau_{21} < 0$, extrema tend to appear over a range of $r = [-11, -1]$; and (5) for $|\alpha_{12}\tau_{21}| > 0.25$, the extrema disappear. These results are valid for $\alpha_{12} = 0.3$ but are only approximations for deviations from this average value of α_{12}. Equation 22 shows that the product $\alpha_{12}\tau_{21}$ can be combined into a new parameter η, so $x_1^M[\eta, r]$, although the range of η is far wider than that of α_{12}.

The equation for inflection points in $\ln\gamma_1$ is

$$\left\{\frac{2x_2[\exp(-\eta) - 1] - 1}{-2x_2 + (2x_2 + 1)\exp(-\eta r)}\right\} = r\left[\frac{x_1 + x_2\exp(-\eta)}{x_2 + x_1\exp(-\eta r)}\right]^4\exp[-2(r-1)\eta] \quad (23)$$

and for $\ln\gamma_2$ it is

$$\left\{\frac{2x_1[1 - \exp(-\eta)] + \exp(-\eta)}{1 + 2x_1[1 - \exp(-\eta r)]}\right\} = r\left[\frac{x_1 + x_2\exp(-\eta)}{x_2 + x_1\exp(-\eta r)}\right]^4\exp[-(2r-1)\eta] \quad (24)$$

Once again it is not practical to provide graphs for this result, as was done for Margules and van Laar. Testing with a graphing calculator shows that NRTL has can provide both single and double inflection points, allowing considerable flexibility in tuning the experiment. Although it can provide single inflections, as shown in Figure 1(a), NRTL, unlike Margules and van Laar, can provide double inflection points on the same graph of ln γ_1 or ln γ_2 vs. x_1. For example, when $\eta = 1.1$ and $r = 1.75$, there are inflection points in ln γ_1 at $x_1 = 0.6610$ and 0.9082 with all values of γ_1 above unity.

Liquid–liquid phase splitting

Again the direct fundamental criteria that $g'' = g''' = 0$ at the onset of phase splitting was used. A ratio of these two criteria applied to the NRTL model results in complex relations between the ratio r and x_1(onset) for fixed values of α_{12}. Although these relations are too complex to be printed here, the positive result is that r is successful in elimination of the two parameters that make up its ratio for the case of phase splitting. Thus graphs of τ_{21}(max) vs. r can be prepared with α_{12} as a parameter. Phase splitting does not occur for $-2 < r < 1$ but can occur when both τ_{12} and τ_{21} are positive or when the first parameter is positive and the second negative. For the latter case, Figure 8(a) shows the single and two liquid phase regions for $r < -2$. Here the value of α_{12} has only a slight effect on phase splitting so a single curve is shown to represent both $\alpha_{12} = 0.3$ and 0.45. Originally, this graph contained also results for $\alpha_{12} = 0$, 0.6 and 0.9 but these have been removed to make the figure easier to read. Generally, a higher value of α_{12} causes the curve of Figure 8(a) to be lowered but for a given value of r the relation between τ_{21}(max) and α_{12} is not always monotonic. Except in rare examples, the reader will not be misled in using the curve of Figure 8(a) for all values of α_{12}.

When both τ_{12} and τ_{21} are positive, Figure 8(b) shows that α_{12} has a significant effect on phase splitting. Here we have included a curve for $\alpha_{12} = 0.6$, although this value is higher than usually encountered. For $\alpha_{12} = 0$, corresponding to the symmetric model, the curve follows $(r + 1)\tau_{21}$ (max) = 2 and thus passes through [1, 1], [3, 0.5], and [5, 1/3] for [r, τ_{21}]. This will aid the reader in interpolation for $0 < \alpha_{12} < 0.3$.

Homogeneous azeotropes

Equation 4 applied to Eq. 21 results in P vs. x_1 diagrams with parameters of r, η, and τ. Previous Figures 4 and 7 would now require another dimension, η. Again with very complex equations we turn to the graphing calculator, which shows a wealth of examples of homogeneous azeotropes, both positive and negative, for the NRTL model. Double azeotropes of both the max/min and min/max type are observed. Triple azeotropes can be found but these cases, as always, should always be checked first for phase splitting, to ensure that the azeotropic composition does not fall in the liquid–liquid gap.

Conclusions

We have examined (1) an extremum and inflection points on the popular ln γ_i vs. x_1 diagram for binary solutions, (2) liquid–liquid phase splitting for binary solutions, and (3) homogeneous azeotropes with three liquid solution models: (a) the two-constant Margules, (b) the van Laar, and (c) the three-constant NRTL models. Then according to ratios of the two constants in the Margules and van Laar models, a series of graphs provides the reader with immediate knowledge of whether phenomena (1)–(3) will occur, given the value of the two constants. As expected, we were only partially successful with the three-constant NRTL model. Here we provided graphs for phase splitting and equations for extrema and inflection points but found no way to represent the results in a two-dimensional graphical form for homogeneous azeotropes nor for extrema and inflection points.

The value of these graphs and equations, and indeed of the article, is that the reader can quickly and easily see whether phenomena (1)–(3) will occur, given the value of the constants

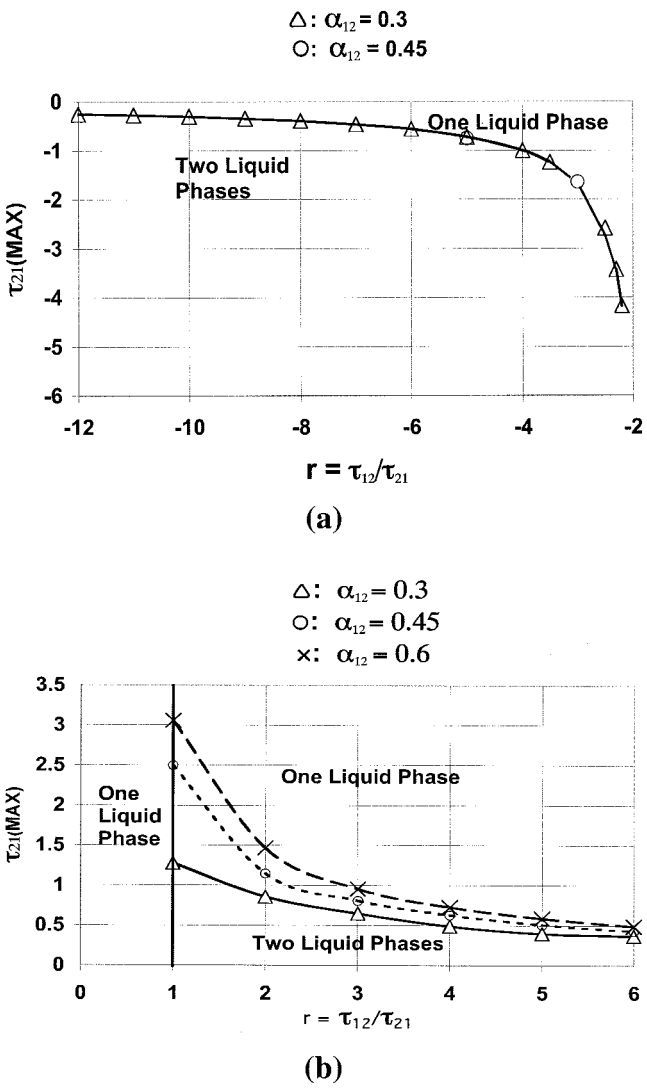

Figure 8. (a) NRTL locus for liquid–liquid phase splitting with $\tau_{12} > \tau_{21}$, with $\tau_{12} > 0$ and $\tau_{21} < 0$. τ_{21}(max) is the maximum value of τ_{21} for which the single-phase liquid splits into two liquid phases for a given value of r. (b) NRTL locus for liquid–liquid phase splitting with $\tau_{12} > \tau_{21}$, with $\tau_{12} > 0$ and $\tau_{21} < 0$. τ_{21}(max) is the maximum value of τ_{21} for which the single-phase liquid splits into two liquid phases for a given value of r.

for the particular liquid model. The first phenomenon may be regarded as a mathematical artifact by some engineers, but the presence of an extremum and inflection points in data for the $\ln \gamma_i$ vs. x_1 diagram tells one something about the least-complicated model that might reasonably represent these data. Here we have shown that data with an extremum should not be fit with a van Laar model equation, whereas both Margules and NRTL models are at least capable of following this phenomenon.

Especially for the last two phenomena is considerable time and effort saved by using these results. For example, why go through a Gibbs minimization calculation only to find the liquid does not split? The same can be said for the homogeneous azeotrope. In both of these examples, where the particular phenomenon is found to exist, from these results the reader should then perform the more detailed calculations to see for (2) the composition of the two liquid phases and for (3) the azeotropic composition and pressure.

Literature Cited

Abbott, M. M., and J. M. Prausnitz, "Modeling the Excess Gibbs Energy," Chapter 1 in *Models for Thermodynamic and Phase Equilibria Calculations*, S. I. Sandler, ed., Marcel Dekker, New York (1994).

Eubank, P. T., and K. R. Hall, "An Equal Area Rule and Algorithm for Determining Phase Compositions," *AIChE J.*, **41**, 924 (1995).

Eubank, P. T., B. G. Lamonte, and J. F. J. Alvarado, "Consistency Tests for Binary VLE Data," *J. Chem. & Eng. Data*, **45**, 1040 (2000).

Gmehling, J., and U. Onken, *Vapor Liquid Equilibrium Data Composition: Aqueous-Organic Systems*, DECHEMA Data Series, **1**(1), Frankfurt, Germany (1977).

Prausnitz, J. M., R. N. Lichtenhaler, and E. Gomes de Azevedo, *Molecular Thermodynamics of Fluid-Phase Equilibria*, 3rd Ed., Prentice Hall, Upper Saddle River, NJ (1999).

Renon, H., and J. M. Prausnitz, "Estimation of Parameters for the NRTL Equation for Excess Gibbs Energies of Strongly Nonideal Liquid Mixtures," *I & EC Proc. Des. & Dev.*, **8**, 413 (1969).

Rowlinson, J. S., and F. L. Swinton, *Liquids and Liquid Mixtures*, 3rd Ed., Butterworths, London (1982).

Sandler, S. I., *Chemical and Engineering Thermodynamics*, 3rd Ed., Wiley, New York (1999).

Smith, J. M., H. C. Van Ness, and M. M. Abbott, *Introduction to Chemical Engineering Thermodynamics*, 6th Ed., McGraw-Hill, New York (2001).

Tester, J. W., and M. Modell, *Thermodynamics and Its Applications*, 3rd Ed., Prentice Hall, Upper Saddle River, NJ (1996).

van Konynenburg, P. H., "Critical Lines and Phase Equilibria in Binary Mixtures," Ph.D. Dissertation, Dept. of Chemistry, UCLA, Los Angeles (1968).

Manuscript received Nov. 26, 2002, and revision received Aug. 21, 2003.